

The Involvement of mGluR5 and TRPV1 in Visceral Nociception In A Rat Model of Uterine Cervical Distension

Wenxin Zhang, PhD¹, Dan Drzymalski, MD², Lihong Sun, MD¹, Qi Xu, MD¹, Cuicui Jiao, MD¹, Luyang Wang, MD¹, Shufang Xie, MD^a, Xiaowei Qian, PhD¹, Hui Wu, PhD¹, Fei Xiao, MD³, Feng FU, MD¹, Ying Feng, MD¹, Xinzhong Chen, PhD¹

¹Women's Hospital, School of Medicine, Zhejiang University, China

²Department of Anesthesiology and Perioperative Medicine, Tufts Medical Center, Boston, MA, USA

³Jiaxing Maternity and Child Care Hospital, China

Corresponding author

Xinzhong Chen, Department of Anesthesia, Women's Hospital, School of Medicine, Zhejiang University, Xueshi Road 1, Hangzhou 310006, China.

E-mail: chenxinz@zju.edu.cn

Abstract Metabotropic glutamate receptor 5 (mGluR5) and transient receptor potential vanilloid subtype 1 (TRPV1) have been shown to play critical roles in the transduction and modulation of cutaneous nociception in the central nervous system. However, little is known regarding the possible involvement of mGluR5 and TRPV1 in regulating visceral nociception from the uterine cervix. In this study, we used a rat model of uterine cervical distension (UCD) to examine the effects of noxious stimuli to the uterine cervix on expression of spinal mGluR5 and TRPV1. Our findings included: (1) UCD resulted in a stimulus-dependent increase in EMG, spinal c-Fos signal, and expression of mGluR5 and TRPV1 in the spinal cord; (2) intrathecal administration of the mGluR5 antagonist 2-methyl-6- (phenylethynyl)-pyridine (MPEP) significantly reduced the increased TRPV1 and c-Fos expression induced by UCD; and, (3) The TRPV1 inhibitor SB-366791 inhibited increased spinal c-Fos expression, but had no effect on the expression of mGluR5 in response to UCD. Our findings indicate that the spinal mGluR5-TRPV1 pathway modulates nociceptive transmission in UCD-induced pathological visceral pain.

Keywords: Visceral nociception; Uterine cervical dilation; TRPV1; mGluR5

Introduction

Metabotropic glutamate receptor 5 (mGluR5) and transient receptor potential vanilloid 1 (TRPV1) channel both play important roles in the transmission of nociceptive stimuli. Studies in mice and rats have demonstrated the role of mGluR5 in the transmission of inflammatory¹⁻³ and neuropathic⁴ pain, and the role of TRPV1 in the transmission of painful chemical and thermal stimuli⁵. The transmission of nociceptive signals can be inhibited by the use of antagonists selective against mGluR5 and TRPV1. 2-methyl-6-(phenylethynyl)-pyridine (MPEP) is a potent, selective mGluR5 antagonist², while N-(3-methoxyphenyl)-4-chlorocinnamide (SB-366791) is a highly potent and selective TRPV1 antagonist⁶.

The role of mGluR5 and TRPV1 in the transmission of visceral pain from the gastrointestinal and urinary systems has been studied in rodent models. MPEP was found to decrease colorectal distension-evoked visceromotor responses in rats, indicating that mGluR5 plays a role in the transmission of visceral nociceptive signals from the gastrointestinal tract⁷. Similarly, *in vitro* experiments using mouse bladders demonstrated that TRPV1 is critical for transmission of stretch-evoked signals⁸, and TRPV1 has also been found to be involved in nociception in the mouse jejunum⁹ and colon¹⁰. It appears that a relationship between TRPV1 and mGluR5 may exist, in which sensitization of TRPV1 through mGluR5 signaling enhances nociceptive stimuli¹¹.

While the role of mGluR5 and TRPV1 in transmitting nociceptive signals in the gastrointestinal and urinary systems has been well characterized, the role in uterine

cervical pain is less well understood. It is known that afferents in the hypogastric nerve originating from the rat uterine cervix express TRPV1¹², and that estrogen may play a role in enhancing the uterine cervical nociceptive signals transmitted by TRPV1¹³. However, the interplay between mGluR5 and TRPV1 during the transmission of painful stimuli during uterine cervical distension (UCD) is unclear.

The aims of this study were to investigate the effects of UCD in a rat model on mGluR5 and TRPV1 expression, and to investigate the effects of MPEP and SB-366791 on the expression of TRPV1 and mGluR5 expression. Our hypothesis was that the expression of mGluR5 and TRPV1 would be increased with UCD, and that MPEP and SB-366791 may decrease TRPV1 and mGluR5 expression.

Materials and Methods

All experimental procedures were carried out in accordance with the National Institute of Health Guide for the Care and Use of Laboratory Animals (NIH Publications No. 86-23). The Animal Ethics and Welfare Committee of the Zhe Jiang University Department of Medicine approved all experimental procedures. Every effort was made to minimize the number of animals used and their suffering.

Animals

A total of 160 Sprague-Dawley-derived adult virgin female rats (Zhejiang Chinese Medical University, Hang Zhou, China, 180-220g) were used. Rats were divided into the following groups: rats subjected to varying degrees of distension forces (5 groups of 18

rats each, n=90), rats treated with antagonists or vehicle (4 groups of 12 rats each, n=48), and control rats (n=16). All rats were allowed one week to acclimate to the house facilities. Rats in whom catheter implantation surgery was planned were housed 1 per cage; all other rats were housed 5 per cage. Rats were kept in a temperature-controlled room (22°C) with free access to food and water and a 12:12-h light-dark cycle. At the end of the experiments all rats were euthanized.

Uterine Cervical Distension Model

A UCD model previously described was modified for the purposes of this study¹⁴. Rats were anesthetized with inhalation of isoflurane (He Bei Yi Pin, China) in oxygen via an isoflurane vaporizer (Matrx, USA) and were maintained with spontaneous ventilation. The concentration of isoflurane was adjusted to 0.7-0.9% so as to allow for detection of rectus abdominus visceromotor response but to prevent spontaneous motor movement. Catheters were inserted into the right carotid artery and vein for blood pressure monitoring and intravenous fluid administration, respectively. A tracheotomy was performed for artificial ventilation. Body temperature was maintained at 37-38°C by a circulating water heating pad throughout the experiment.

Once the rats were anesthetized, a 1.5cm midline lower abdominal incision was made to expose the uterus. All incisions were infiltrated with lidocaine (He Bei Yi Pin, China). Two sterilized fine metal rods (23G needles, RWD Life Science, China) were inserted through the cervical os, with one end entering the uterus through the abdominal incision and the other end exiting through the upper vaginal wall. Each rod was connected to a 1-0

silk suture, with one end attached to a metal stand and the other end connected to a pulley system for application of manual weighted traction. Each rat was then subjected to UCD with a distension force of 0, 25, 50, 75 or 100g. To simulate contractions occurring at regular intervals during labor, distension forces were applied for 20 seconds every 3 minutes for a total duration of 1 hour. Following UCD, a 30-minute recovery period was allowed prior to subsequent procedures. The submaximal distension force of 75g was the only force applied in rats that had drug or vehicle administration.

Visceromotor Responses

The visceromotor response to UCD was quantified using electromyographic (EMG) recordings from the rat rectus abdominus muscle. Two concentric monitoring needle electrodes (Mei Yi, Nan Jing, China) were inserted into the rectus abdominus muscle immediately after placement of the UCD rods. The baseline EMG amplitude was measured for 10 minutes, after which visceromotor responses were recorded throughout the entire hour of UCD. Physiological measurements, including electrocardiography and blood pressure, were also recorded by a MedLab biological signal acquisition system (Mei Yi, Nan Jing, China). The EMG signal was amplified and filtered at 3000 Hz, and raw data were then integrated and digitized by calculating the area under the curve. Following measurement of the raw EMG amplitude during the 20 seconds of each distension cycle, the net EMG amplitude was calculated by subtracting the mean EMG amplitude during the first 20 seconds after each distention ceased from the raw EMG amplitude.

Intrathecal Catheter Placement

A previously described method for insertion of an intrathecal catheter was used¹⁵ for those rats that underwent intrathecal catheter placement. After anesthetizing the rats with an intraperitoneal injection of 60mg/kg sodium pentobarbital (He Bei Yi Pin, China), a midline incision at the atlanto-occipital junction was made. A fine bore polyethylene-10 catheter (Smiths Medical, USA) filled with 0.9% sterile saline was passed through the dura and into the subarachnoid space. The catheter was advanced 7.5 cm caudally such that the tip was placed at the level of the lumbar enlargement, while the cephalic portion of the catheter was secured at the neck. Three days after intrathecal catheter placement, catheter position was verified by injecting 2mg/kg of 2% lidocaine (He Bei Yi Pin, China). Rats were given 5-7 days to recover after intrathecal catheter placement. If signs of motor impairment were present, rats were immediately euthanized.

Drugs

MPEP and SB-366791 (Selleck Chemicals, USA) were dissolved in 5% dimethyl sulfoxide (DMSO) (Sigma-Aldrich, USA) to a concentration of 20nmol/ μ l. Thirty minutes prior to UCD, MPEP (30 μ g in 25 μ l) or SB-366791 (30 μ g in 25 μ l) was administered intrathecally via micro syringe (Shanghai High Pigeon, China) in those rats that were randomized to receive the mGluR5 and TRPV1 inhibitors. Rats randomized to vehicle treatment received 25 μ l DMSO in the same manner, while rats randomized to the

control group received no drug via intrathecal catheter. Following administration of the drug or vehicle, 5 μ l saline was injected to ensure complete delivery. MPEP and SB-366791 dosing was based on previous reports¹⁶⁻¹⁸. The dose of DMSO was based on previous studies that demonstrated a lack of noxious effect on spinal cord neurons at this dose². Unless otherwise specified, chemical reagents were HPLC grade and purchased from Sinopharm Chemical Reagent.

Tissue Preparation

After the experiments, rats were euthanized and incisions were made on both sides of the vertebral column. The tissues were dissected and the area of the lumbar enlargement of the spinal cord encompassing the T12-L2 segments was removed under aseptic condition. All samples were then fast-frozen in liquid nitrogen and stored at -80°C.

Western Blot Experiments

The tissues were homogenized using mortars and pestles in an ice-cold lysis buffer (1% NP-40, 0.5% Sodium deoxycholate, 0.1% SDS, Boster, Wu Han, China) with freshly added protease inhibitor cocktail tablets (Roche Diagnostics, USA). Following 30 minutes of incubation, the liquid was centrifuged at 12000 rpm at 4°C for 20 minutes. The supernatant was collected and the protein concentration was calculated using the Bicinchoninic acid method according to the manufacturer's instructions (KeyGen Biotech, Nan Jing, China). An equivalent amount of protein (30 μ g) and prestained protein ladder (ThermoFisher Scientific, USA) was loaded on a 12% SDS polyacrylamide gel

(Invitrogen, ThermoFisher Scientific, USA). Electrophoresis was run for 50 minutes at 200V, after which the protein was transferred to polyvinylidene fluoride membranes (Millipore, USA) and the blots were blocked with 5% non-fat milk in Tris-buffered saline for two hours at room temperature. The blots were then incubated with primary antibodies at 4°C overnight. The antibodies used included: anti- β -actin antibody (rabbit affinity purified polyclonal antibody; 1:3000, Abcam, Hong Kong, China), anti-mGluR5 antibody (rabbit affinity purified monoclonal antibody; 1:5000, Abcam, Hong Kong, China), and anti-TRPV1 antibody (Anti-Rat TRPV1 antibody; 1:200, Alomone, Isreal). Blots were washed and incubated with HRP-conjugated secondary antibody (1:8000, Boster, Wu Han, China) for 2 hours at room temperature. All antibodies were diluted in blocking buffer. Immunoblots were detected with an enhanced chemiluminescence kit (Millipore, USA) and visualized on GeneSnap image acquisition software (Syngene, UK). The density of the bands was quantified using densitometric analysis on Quantity One software (Bio-Rad, USA). The intensity of mGluR5 or TRPV1 bands was normalized to their β -actin intensity.

Quantitative Real-Time Reverse-Transcription Polymerase Chain Reactions

Total RNA was isolated from the frozen lumbar spinal cord enlargement using Trizol reagent (Life Technologies, CA, USA). RNA concentration was measured with the NanoDrop ND-1000 Spectrometer (NanoDrop Technologies, Wilmington, DE). Two-step reverse transcription-polymerase chain reaction (RT-PCR) was performed using reagents and kits from Takara (Takara, China). Starting with 2.5 μ g of total RNA,

PCR amplification was performed using a SYBR PrimeScript Quantitative Real-Time RT-PCR Kit (Takara, China) according to the manufacturer's instruction. The specific forward and reverse primers are shown in Table 1.

The selected primers amplify all known splice variants of mGluR5. PCR amplification was performed on the CFX96 Real-Time PCR Detection System (Bio-Rad, USA). Relative changes in mGluR5 and TRPV1 messenger RNA levels were calculated using the $\Delta\Delta C_t$ method, and the reference gene β -actin was used as a normalizer. Reactions without any template were included as negative controls.

Immunohistochemistry

Rats were perfused transcardially with 4% paraformaldehyde at 4°C for the immunohistochemistry experiments. Tissue removed from perfused animals was then post-fixed for 5 hours in 4% paraformaldehyde, and then cryoprotected overnight in 30% sucrose in phosphate-buffered saline (PBS) at 4°C. Tissue was cryosectioned (8 μ m), mounted on microscope slides, incubated with normal goat serum (Boster, WuHan, China) in PBS for 2 hours to block non-specific staining, and finally incubated with primary antibodies (rabbit polyclonal anti-c-Fos antibody, SantCruz, USA) at 4°C overnight. The sections were then washed in PBS and incubated with FITC-conjugated goat anti-rabbit antibody (Beyotime, Shanghai, China) for 30 minutes at room temperature. In the control experiments, tissues were processed using the same staining protocol, but without applying the primary antibodies. For co-localization of mGluR5 and TRPV1 in the spinal cord, fluorescent probes (Anti-Rat-TRPV1-ATTO-488, 1:50, Anti-mGluR5-ATTO-594,

1:50, Alomone, Isreal) were applied simultaneously to the sections. Coverslips were mounted using Antifade Mounting Medium (Beyotime, Shanghai, China) and viewed using a fluorescence microscope (Eclipse Ni-E, Nikon, Shanghai, China). Images were analyzed using the Image J 1.50i (National Institute of Health, USA). On the images, a line was drawn surrounding the area of spinal lamina III-V and an observer blinded to the groups counted the number of fos-positive neurons within this region. The total number of nuclei in the same area was calculated, and the proportion of fos-positive neurons to the number of nuclei of the same region is presented in the results.

Statistical Analysis

Data are expressed as mean \pm SD. PCR and Western blot data after UCD were analyzed by one-way ANOVA for overall differences among groups, with Bonferroni's multiple comparisons test for pairwise comparisons. The semi-quantified data of spinal c-fos expression in each group were compared using 2-tail paired student t-test. Statistical analysis was performed using SPSS Statistics Version 22.0 (IBM Corporation, Armonk, NY). $P < 0.05$ was considered statistically significant.

RESULTS

Effect of UCD on spinal mGluR5 expression

The mGluR5 antibody detected a Western blot band at 137kDa, while the β -actin antibody detected a Western blot band at 45kDa (fig. 1A). The integrated optical density

(IOD) ratio of each band was determined and fold increase in IOD is presented in the figures. UCD significantly increased spinal mGluR5 mRNA and protein expression in a stimulus intensity-dependent manner (fig. 1B and 1C). The immunohistochemistry results also demonstrated that the change in spinal mGluR5 levels was primarily found in the deep dorsal horn (lamina III~V) region of the spinal cord. While lamina I and II expressed dense mGluR5, its expression did not change significantly between the stimulated and sham groups (fig. 1D).

Effect of UCD on spinal TRPV1 expression

The TRPV1 antibody detected a Western blot band at 97kDa, while the β -actin antibody detected a Western blot band at 45kDa (fig. 2A). The IOD ratio of each band was determined and fold increase in IOD is presented in the figures. UCD significantly increased spinal TRPV1 mRNA and protein expression in a stimulus intensity-dependent manner (fig. 2B and 2C). The immunohistochemistry results also showed that the change in spinal TRPV1 levels was primarily found in the deep dorsal horn (lamina III-V) region of the spinal cord. Lamina I and II expressed dense TRPV1, but its expression did not change significantly between the stimulated and sham groups (fig. 2D).

Effect of MPEP on TRPV1 and SB-366791 on mGluR5 in rats undergoing UCD

Spinal TRPV1 mRNA and protein expression by Western blot was significantly reduced in rats that had intrathecal administration of MPEP prior to UCD (fig. 3A, B, C). Intrathecal administration of MPEP did not have a significant effect on protein or mRNA

expression of mGluR5 (fig. 3D, E, F). Spinal mGluR5 protein expression and its mRNA level were similar in rats with intrathecal administration of SB-366791, control, and vehicle (fig. 4). There was no significant difference in the expression of TRPV1 between those rats that had intrathecal injection of DMSO or no drug (fig. 3).

Localization of mGluR5 and TRPV1 receptors in rat spinal cord

In rats subjected to a distension force of 75g, cells expressing both mGluR5 and TRPV1 located densely in the deep dorsal horn region (lamina III-V) (fig. 5). In addition, mGluR5 and TRPV1 were expressed in naïve rat spinal cord, with the most dense expression in lamina I-II of the dorsal horn. Neurons co-expressing mGluR5 and TRPV1 in lamina I-II of the spinal cord in both sham and UCD treated rats were also detected (fig. 9).

Validation of UCD model by measurement of spinal c-Fos expression and EMG

Deep dorsal horn c-Fos expression in response to UCD was observed on immunofluorescence (fig. 6A). Expression quantification demonstrated a stimulus intensity-dependent increase of c-Fos positive neurons, and the changes concentrated mainly around lamina III-V of the spinal cord (fig. 6A, B). Increasing UCD forces also resulted in increased EMG signal intensity (fig. 6C, D). In rats treated with MPEP or SB-366791, deep dorsal horn (lamina III-V) c-Fos expression on immunofluorescence as well as the EMG signal was significantly reduced compared with the DMSO-treated

group (fig. 7, 8). Negative controls without incubation of the first antibodies produced no signal (fig. 10).

DISCUSSION

In this study, we found that UCD in rats results in increased spinal mGluR5 and TRPV1 mRNA and protein expression in a stimulus intensity-dependent manner. We also found that intrathecal administration of MPEP 30 minutes prior to UCD results in decreased spinal TRPV1 mRNA and protein expression, while intrathecal administration of SB-366791 30 minutes prior to UCD did not affect spinal mGluR5 mRNA and protein expression. Finally, we found that cells expressing changes in both mGluR5 and TRPV1 located most densely to the deep dorsal horn region.

The finding that mGluR5 and TRPV1 expression was increased with UCD is not surprising, as similar results have been found in gastrointestinal and urinary models of visceral pain. mGluR5 has been implicated in playing a role in the transmission of visceral pain in a colorectal distension rat model⁷. TRPV1 has also been shown to play an important role in the transmission of stretch-evoked nociceptive signals in the bladder⁸. Our study further confirms that mGluR5 and TRPV1 play a role in the transmission of nociceptive signals in many viscera, including the uterine cervix.

Our finding that the effect of UCD exerted on neuronal transmission occurs within such a rapid time frame is consistent with other models of acute visceral nociception (e.g. 70 minutes in colorectal distension and 1 hour in bladder distension models^{7,8}). Furthermore, spinal protein kinase A (PKA) levels increase in a stimulus-dependent manner after

intra-colonic noxious stimulation within a timeframe of 60 minutes²⁵, and the mGluR1/5 agonist DHPG enhances TRPV1 phosphorylation in a protein kinase C (PKC)-dependent manner within a timeframe of 45 minutes in dissociated rat trigeminal ganglion neurons¹⁹. Given that PKA and PKC are downstream messengers of mGluR5 and potential TRPV1 modulators, these results further support our findings that the rapid effect of acute visceral nociception in our UCD model on mGluR5 and TRPV1 expression are valid.

Decreased levels of TRPV1 were found in MPEP treated rats, but no change in mGluR5 expression was demonstrated in SB-366791 treated rats, suggesting that mGluR5 may be an upstream regulator of TRPV1 expression in uterine cervical nociception. This finding is supported by prior studies that have suggested mGluR5 activation results in phosphorylation-induced sensitization of TRPV1, thereby enhancing thermal and mechanical hyperalgesia^{11,19}. Similarly, other studies have found that activation of spinal mGluR5 elicits Ca²⁺ influx via the non-selective cation channel TRPV1^{20,21}.

Our findings offer a more extensive understanding of the interplay between mGluR5 and TRPV1. First, the finding that mGluR5 and TRPV1 co-localized in the deep dorsal horn in rats subjected to UCD suggests that TRPV1 and mGluR5 may be coupled in the sensory neurons of the spinal cord. Second, the finding that TRPV1 mRNA expression was significantly decreased by MPEP suggests that mGluR5 participates pre-translationally. Such a theory is supported by an electrophysiological study performed by Hu et al., which demonstrated that activation of mGluR5 enhanced TRPV1 expression via protein kinase A and cyclooxygenase pathways²². Finally, our results

suggest that mechanical hypersensitivity during uterine cervical distension may be modulated by mGluR5 through regulation of TRPV1. This idea is supported by Chung et al.¹⁹, who demonstrated that mGluR5 activation results in enhanced mechanical hyperalgesia through TRPV1 phosphorylation in trigeminal sensory neurons.

Our study has several important limitations. First, while MPEP has mGluR5 inhibitor properties, it also expresses NMDA receptor antagonist properties²³. Given that activation of NMDA receptors sensitizes TRPV1 channels²⁴, we cannot definitively determine if MPEP resulted in a decrease in TRPV1 through decreasing mGluR5 or NMDA expression. Second, MPEP retains analgesic properties in mGluR5 knockout mice³, thus questioning whether our results may have been influenced by its actions on the NMDA receptor. Finally, locomotor side effects have been associated with the use of MPEP, which may limit clinical utility².

Despite these limitations, one of the most important strengths of our study is that we had a well-functioning UCD model for investigating visceral pain originating from the uterine cervix. We modified the UCD rat model developed by Tong et al.¹⁴ by using a lighter depth of anesthesia that prevented purposeful escape but still allowed for detection of rectus abdominus visceromotor responses. The validation experiments demonstrated that UCD resulted in a stimulus intensity-dependent increase in EMG and spinal c-Fos, and a decrease in EMG and spinal c-Fos in the setting of antagonist administration, indicating that our UCD model successfully elicited visceral pain at the uterine cervix.

In summary, our study demonstrates that UCD stimulates spinal mGluR5 and TRPV1 expression, MPEP decreases TRPV1 expression, but SB-366791 does not change

mGluR5 expression. These results suggest that mGluR5 and TRPV1 may play an important role in the modulation of nociceptive signals during uterine contractions, and that mGluR5 may be an upstream regulator of TRPV1 expression. Further studies are needed to better understand the role these and other receptors and channels play in the transmission of visceral nociception during labor.

Abbreviations

mGluR5, metabotropic glutamate receptor 5; TRPV1, transient receptor potential vanilloid subtype 1; UCD, uterine cervical distension; MPEP, 2-methyl-6-(phenylethynyl)-pyridine; CRD, colorectal distension; DMSO, dimethyl sulfoxide.

Competing interests

The authors declare no competing interests.

Authors' contributions

- Xinzhong Chen designed the experiments in this study and drafted the manuscript.
- Wenxin Zhang performed the experiments and data analysis.
- Lihong Sun performed the experiments and data analysis.
- Qi Xu, Hui Wu performed the experiments and data analysis.
- Dan Drzymalski performed revisions and contributed to the intellectual development of the manuscript.
- Cuicui Jiao contributed to the design of the study and approved the final manuscript.

- Luyang Wang contributed to the design of the study and approved the final manuscript.
- Shufang Xie contributed to the design of the study and approved the final manuscript.
- Fei Xiao contributed to the design of the study and approved the final manuscript.
- Feng Fu contributed to the design of the study and approved the final manuscript.
- Ying Feng contributed to the design of the study and approved the final manuscript.
- Xiaowei Qian contributed to the design of the study and approved the final manuscript.

Acknowledgments

This study was supported by funding from the National Natural Science Foundation of China (NSFC, No. 81271237, No. 81471126 and No. 81501702.), and the Zhejiang Provincial Natural Foundation of China under grant No. LY15H150007. The authors would like to thank Professor Shucui Ling (Zhejiang University School of Medicine, Zhejiang, China) for his technological guidance in the experiments performed as part of this study.

Author details

^aDepartment of Anesthesia, Women's Hospital, School of Medicine, Zhejiang University, Hangzhou, Zhejiang Province, China.^[1]^[2]^[3]

^bDepartment of Anesthesiology and Perioperative Medicine, Tufts Medical Center, Boston, Massachusetts, United States of America

^cDepartment of Anesthesia, Jiaxing Maternity and Child Care Hospital, Jiaxing, Zhejiang 314005, China

REFERENCES

1. Karim F, Wang CC and Gereau RWt. Metabotropic glutamate receptor subtypes 1 and 5 are activators of extracellular signal-regulated kinase signaling required for inflammatory pain in mice. *The Journal of neuroscience : the official journal of the Society for Neuroscience* 2001; 21: 3771-3779. 2001/05/23.
2. Zhu CZ, Wilson SG, Mikusa JP, Wismer CT, Gauvin DM, Lynch JJ, 3rd, Wade CL, Decker MW and Honore P. Assessing the role of metabotropic glutamate receptor 5 in multiple nociceptive modalities. *European journal of pharmacology* 2004; 506: 107-118. 2004/12/14. DOI: 10.1016/j.ejphar.2004.11.005.
3. Montana MC, Cavallone LF, Stubbert KK, Stefanescu AD, Kharasch ED and Gereau RWt. The metabotropic glutamate receptor subtype 5 antagonist fenobam is analgesic and has improved in vivo selectivity compared with the prototypical antagonist 2-methyl-6-(phenylethynyl)-pyridine. *The Journal of pharmacology and experimental therapeutics* 2009; 330: 834-843. 2009/06/12. DOI: 10.1124/jpet.109.154138.
4. Fisher K, Lefebvre C and Coderre TJ. Antinociceptive effects following intrathecal pretreatment with selective metabotropic glutamate receptor compounds in a rat model of neuropathic pain. *Pharmacology, biochemistry, and behavior* 2002; 73: 411-418. 2002/07/16.
5. Caterina MJ, Leffler A, Malmberg AB, Martin WJ, Trafton J, Petersen-Zeitze KR, Koltzenburg M, Basbaum AI and Julius D. Impaired nociception and pain sensation in mice lacking the capsaicin receptor. *Science (New York, NY)* 2000; 288: 306-313. 2000/04/15.
6. Gunthorpe MJ, Rami HK, Jerman JC, Smart D, Gill CH, Soffin EM, Luis Hannan S, Lappin SC, Egerton J, Smith GD, Worby A, Howett L, Owen D, Nasir S, Davies CH, Thompson M, Wyman PA, Randall AD and Davis JB. Identification and characterisation of SB-366791, a potent and selective vanilloid receptor (VR1/TRPV1) antagonist. *Neuropharmacology* 2004; 46: 133-149. 2003/12/05.
7. Lindstrom E, Brusberg M, Hughes PA, Martin CM, Brierley SM, Phillis BD, Martinsson R, Abrahamsson C, Larsson H, Martinez V and Blackshaw LA. Involvement of metabotropic glutamate 5 receptor in visceral pain. *Pain* 2008; 137: 295-305. 2007/10/17. DOI: 10.1016/j.pain.2007.09.008.
8. Birder LA, Nakamura Y, Kiss S, Nealen ML, Barrick S, Kanai AJ, Wang E, Ruiz G, De Groat WC, Apodaca G, Watkins S and Caterina MJ. Altered urinary bladder function in mice lacking the vanilloid receptor TRPV1. *Nature neuroscience* 2002; 5: 856-860. 2002/08/06. DOI: 10.1038/nn902.
9. Rong W, Hillsley K, Davis JB, Hicks G, Winchester WJ and Grundy D. Jejunal afferent nerve sensitivity in wild-type and TRPV1 knockout mice. *The Journal of physiology* 2004; 560: 867-881. 2004/08/28. DOI: 10.1113/jphysiol.2004.071746.
10. Jones RC, 3rd, Xu L and Gebhart GF. The mechanosensitivity of mouse colon afferent fibers and their sensitization by inflammatory mediators require transient

- receptor potential vanilloid 1 and acid-sensing ion channel 3. *The Journal of neuroscience : the official journal of the Society for Neuroscience* 2005; 25: 10981-10989. 2005/11/25. DOI: 10.1523/jneurosci.0703-05.2005.
11. Honda K, Shinoda M, Kondo M, Shimizu K, Yonemoto H, Otsuki K, Akasaka R, Furukawa A and Iwata K. Sensitization of TRPV1 and TRPA1 via peripheral mGluR5 signaling contributes to thermal and mechanical hypersensitivity. *Pain* 2017; 158: 1754-1764. 2017/06/18. DOI: 10.1097/j.pain.0000000000000973.
12. Tong C, Conklin D, Clyne BB, Stanislaus JD and Eisenach JC. Uterine cervical afferents in thoracolumbar dorsal root ganglia express transient receptor potential vanilloid type 1 channel and calcitonin gene-related peptide, but not P2X3 receptor and somatostatin. *Anesthesiology* 2006; 104: 651-657. 2006/03/31.
13. Yan T, Liu B, Du D, Eisenach JC and Tong C. Estrogen amplifies pain responses to uterine cervical distension in rats by altering transient receptor potential-1 function. *Anesthesia and analgesia* 2007; 104: 1246-1250, tables of contents. 2007/04/26. DOI: 10.1213/01.ane.0000263270.39480.a2.
14. Tong C, Ma W, Shin SW, James RL and Eisenach JC. Uterine cervical distension induces cFos expression in deep dorsal horn neurons of the rat spinal cord. *Anesthesiology* 2003; 99: 205-211. 2003/06/27.
15. Yaksh TL and Rudy TA. Chronic catheterization of the spinal subarachnoid space. *Physiology & behavior* 1976; 17: 1031-1036. 1976/12/01.
16. Ren BX, Gu XP, Zheng YG, Liu CL, Wang D, Sun YE and Ma ZL. Intrathecal injection of metabotropic glutamate receptor subtype 3 and 5 agonist/antagonist attenuates bone cancer pain by inhibition of spinal astrocyte activation in a mouse model. *Anesthesiology* 2012; 116: 122-132. 2011/11/30. DOI: 10.1097/ALN.0b013e31823de68d.
17. Varty GB, Grilli M, Forlani A, Fredduzzi S, Grzelak ME, Guthrie DH, Hodgson RA, Lu SX, Nicolussi E, Pond AJ, Parker EM, Hunter JC, Higgins GA, Reggiani A and Bertorelli R. The antinociceptive and anxiolytic-like effects of the metabotropic glutamate receptor 5 (mGluR5) antagonists, MPEP and MTEP, and the mGluR1 antagonist, LY456236, in rodents: a comparison of efficacy and side-effect profiles. *Psychopharmacology* 2005; 179: 207-217. 2005/02/01. DOI: 10.1007/s00213-005-2143-4.
18. Xu T, Jiang W, Du D, Xu Y, Zhou Q, Pan X, Lou Y, Xu L and Ma K. Inhibition of MPEP on the development of morphine antinociceptive tolerance and the biosynthesis of neuronal nitric oxide synthase in rat spinal cord. *Neuroscience letters* 2008; 436: 214-218. 2008/04/09. DOI: 10.1016/j.neulet.2008.03.028.
19. Chung MK, Lee J, Joseph J, Saloman J and Ro JY. Peripheral group I metabotropic glutamate receptor activation leads to muscle mechanical hyperalgesia through TRPV1 phosphorylation in the rat. *The journal of pain : official journal of the American Pain Society* 2015; 16: 67-76. 2014/12/03. DOI: 10.1016/j.jpain.2014.10.008.

20. Kim YH, Park CK, Back SK, Lee CJ, Hwang SJ, Bae YC, Na HS, Kim JS, Jung SJ and Oh SB. Membrane-delimited coupling of TRPV1 and mGluR5 on presynaptic terminals of nociceptive neurons. *The Journal of neuroscience : the official journal of the Society for Neuroscience* 2009; 29: 10000-10009. 2009/08/14. DOI: 10.1523/jneurosci.5030-08.2009.
21. Cartmell J and Schoepp DD. Regulation of neurotransmitter release by metabotropic glutamate receptors. *Journal of neurochemistry* 2000; 75: 889-907. 2000/08/11.
22. Hu HJ, Bhawe G and Gereau RWt. Prostaglandin and protein kinase A-dependent modulation of vanilloid receptor function by metabotropic glutamate receptor 5: potential mechanism for thermal hyperalgesia. *The Journal of neuroscience : the official journal of the Society for Neuroscience* 2002; 22: 7444-7452. 2002/08/28.
23. O'Leary DM, Movsesyan V, Vicini S and Faden AI. Selective mGluR5 antagonists MPEP and SIB-1893 decrease NMDA or glutamate-mediated neuronal toxicity through actions that reflect NMDA receptor antagonism. *British journal of pharmacology* 2000; 131: 1429-1437. 2000/11/23. DOI: 10.1038/sj.bjp.0703715.
24. Lee J, Chung MK and Ro JY. Activation of NMDA receptors leads to phosphorylation of TRPV1 S800 by protein kinase C and A-Kinase anchoring protein 150 in rat trigeminal ganglia. *Biochemical and biophysical research communications* 2012; 424: 358-363. 2012/07/14. DOI: 10.1016/j.bbrc.2012.07.008.
25. Jing Wua,+, Guangxiao Sub,+, Long Mab, Xuan Zhang c, Yongzhong Leib, Qing Linc, Haring J.W. Nautab, Junfa Lid, and Li Fangb,c. The role of c-AMP-dependent protein kinase in spinal cord and post synaptic dorsal column neurons in a rat model of visceral pain. *Neurochemistry international* 2007; 50(5): 710-718.. 2007/10/19. DOI:10.1016/j.neuint.2007.01.006

	Forward Primer	Reverse Primer
mGlu R5	AGCAGATCCAGCAGCCTAGTCAA	GACAGACAGTCGCTGCCACA A
TRPV	GAAGCAGTTTGTCAATGCCAGCT	AGGGTCACCAGCGTCATGTT

1	A	C
β -actin	AGGTCGGTGTGAACGGATTTG	GGGGTCGTTGATGGCAACA

Table 1. Forward and Reverse Primers of mGluR5, TRPV1, and β -actin

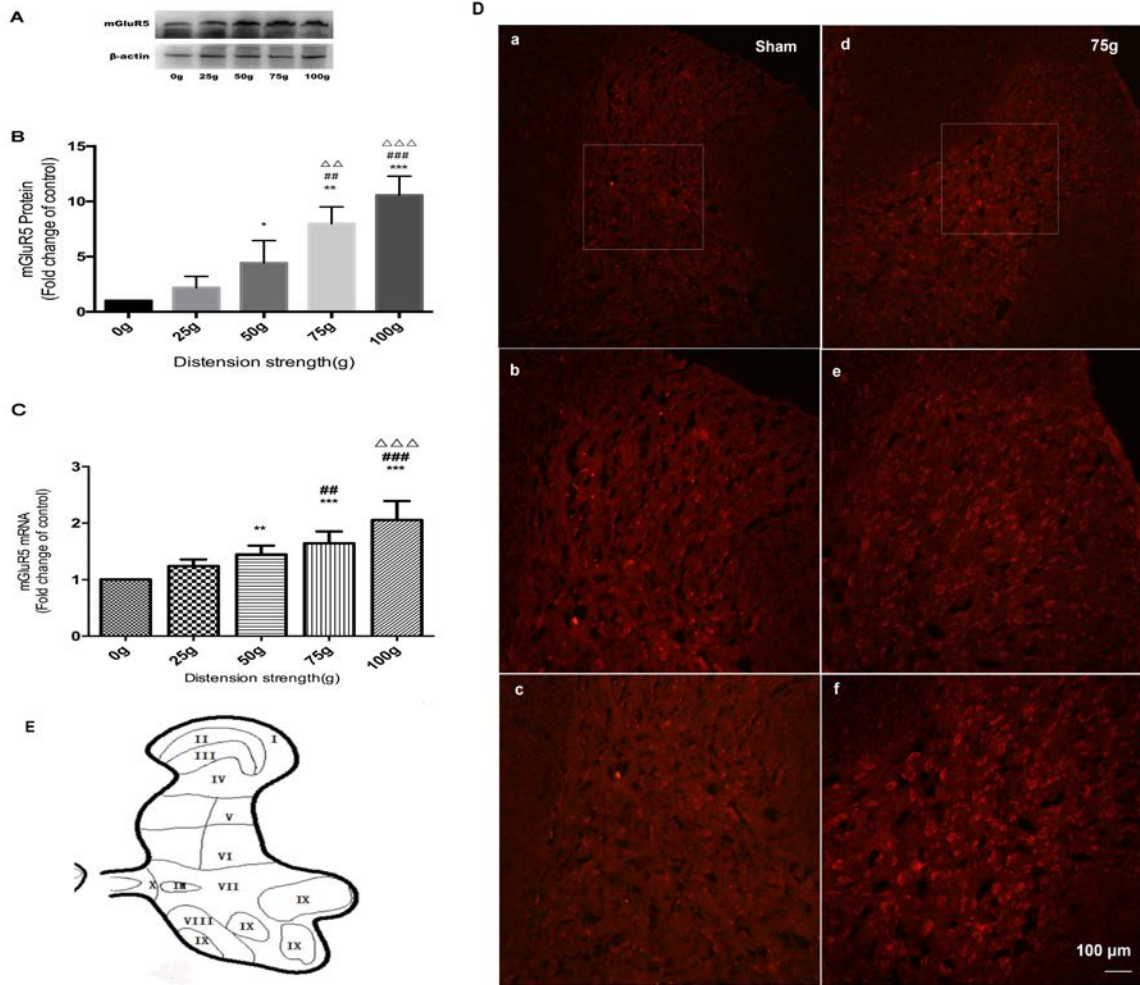


Figure 1

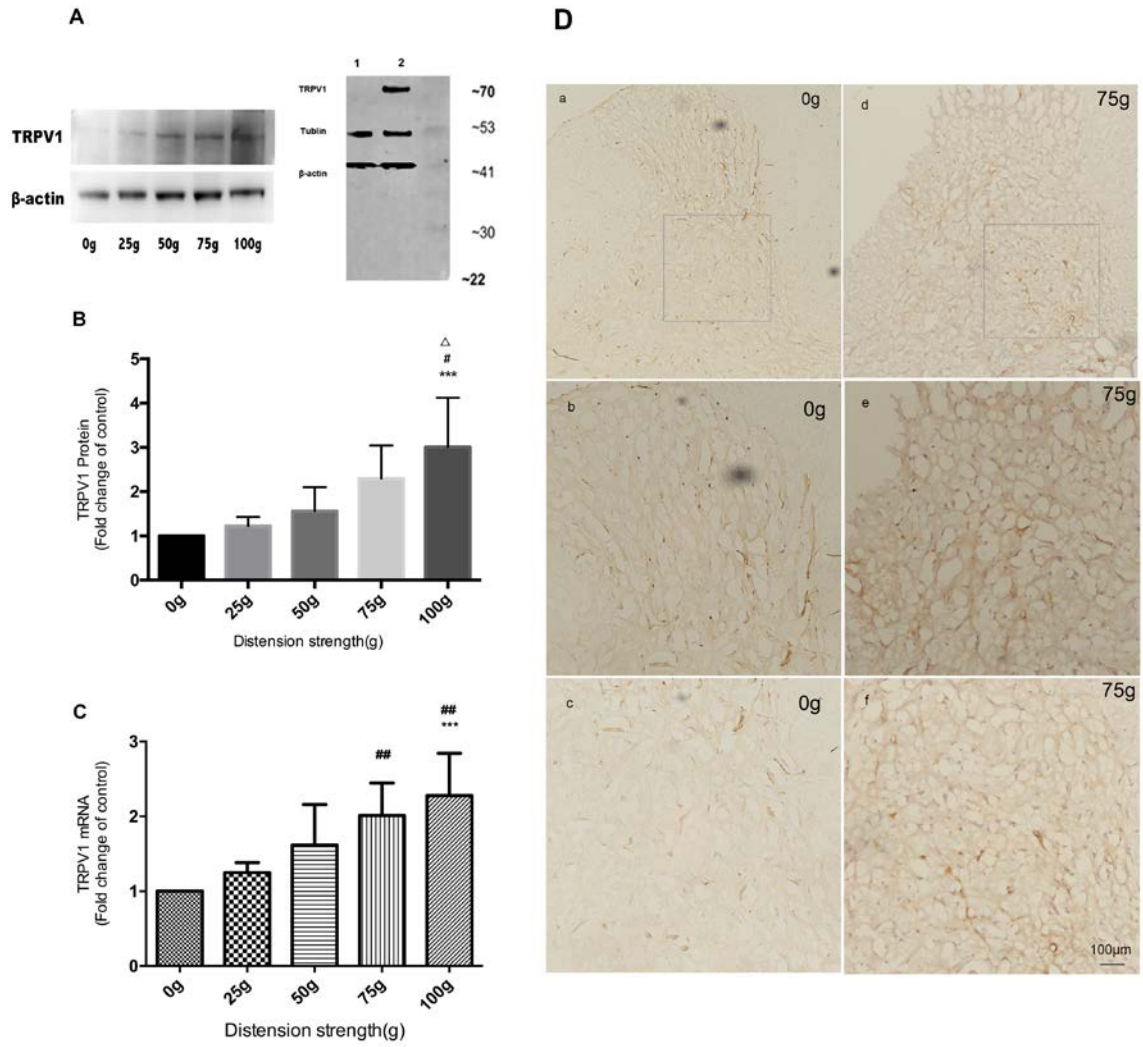


Figure 2

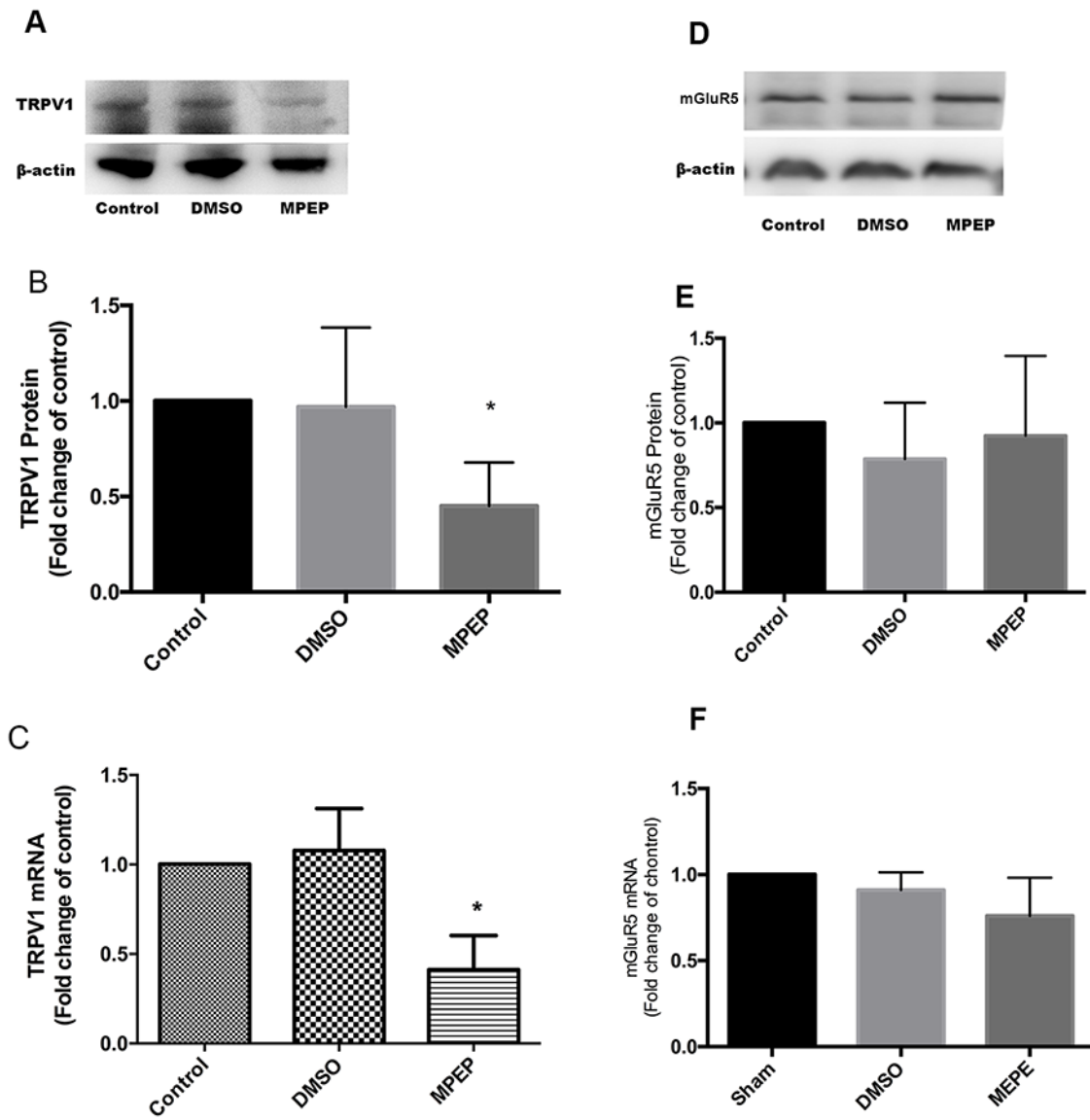


Figure 3

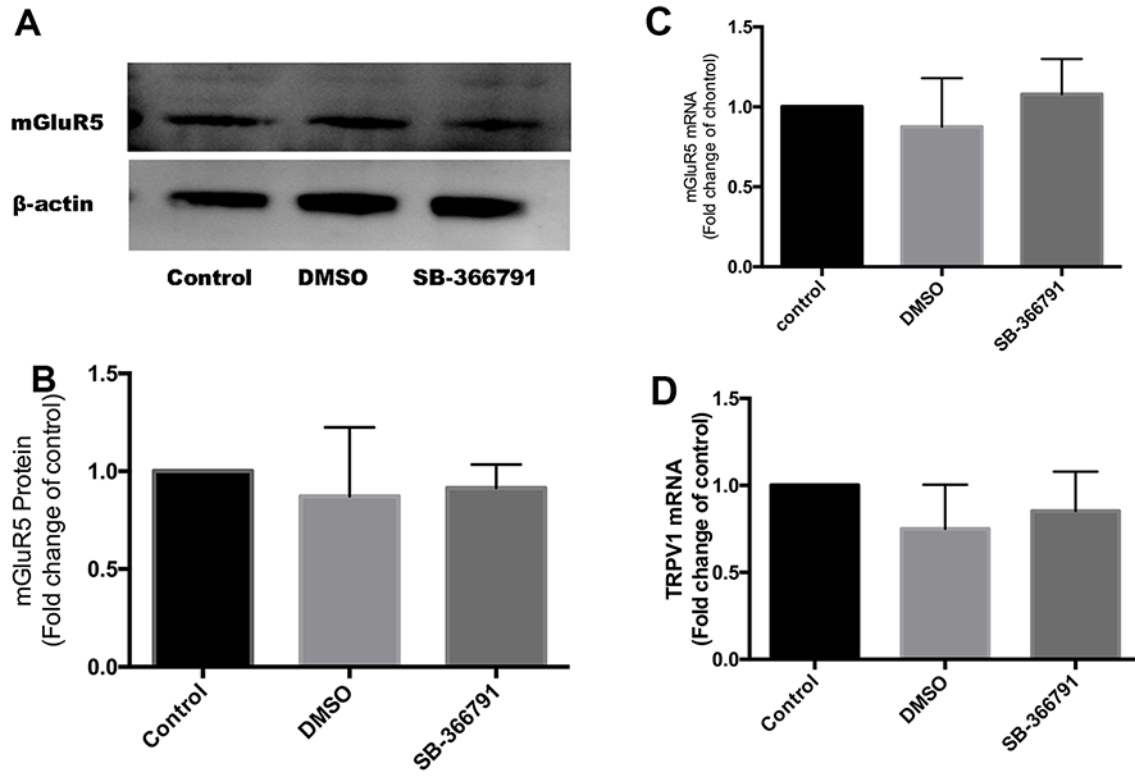


Figure 4

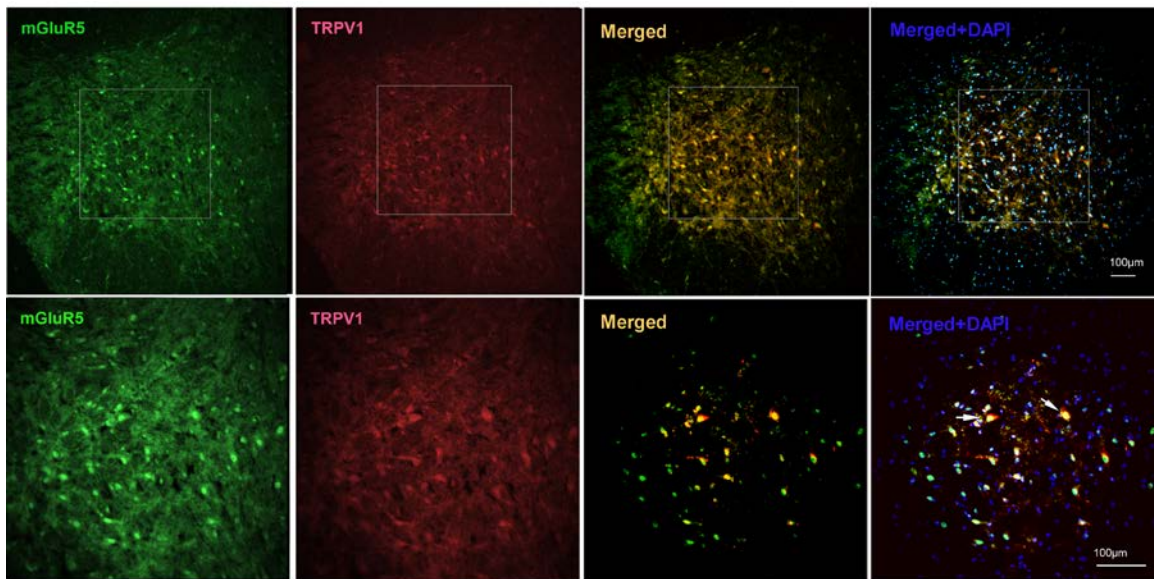


Figure 5

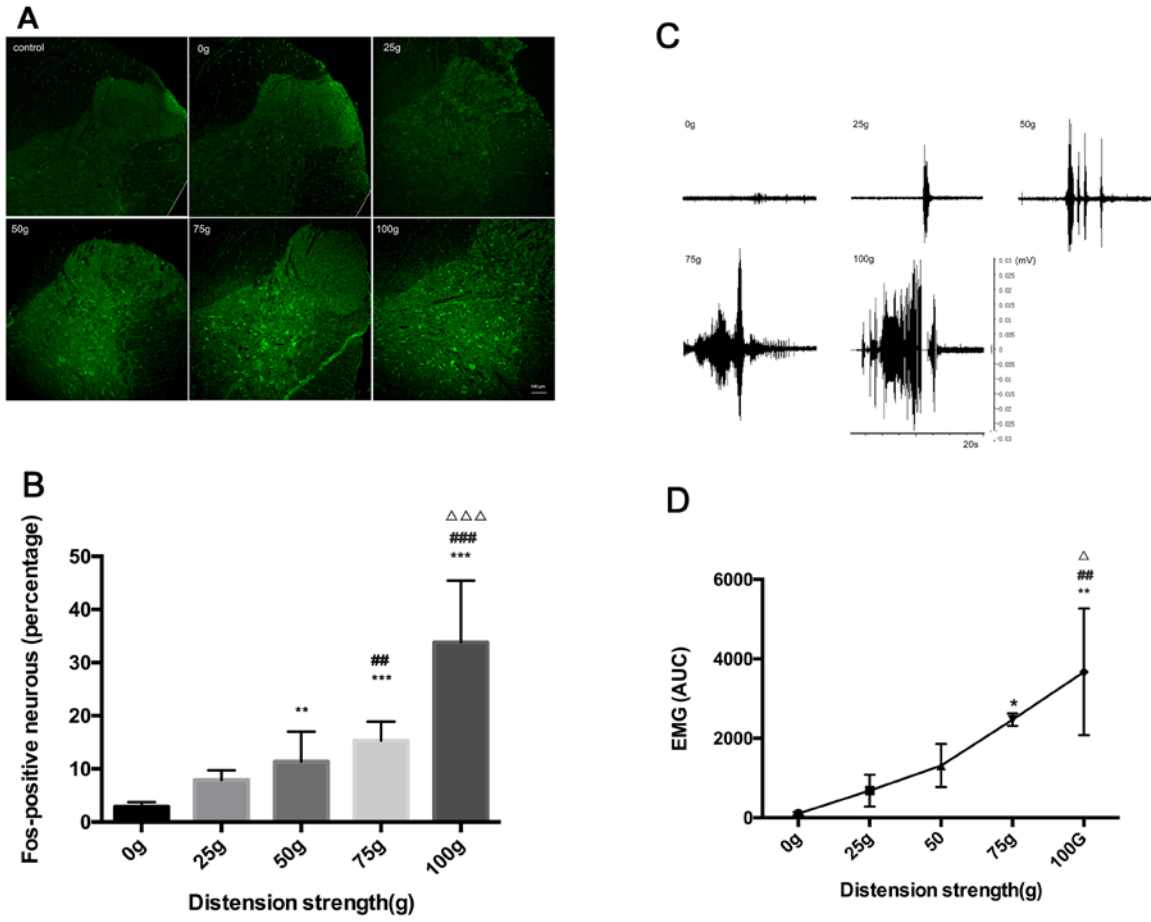


Figure 6

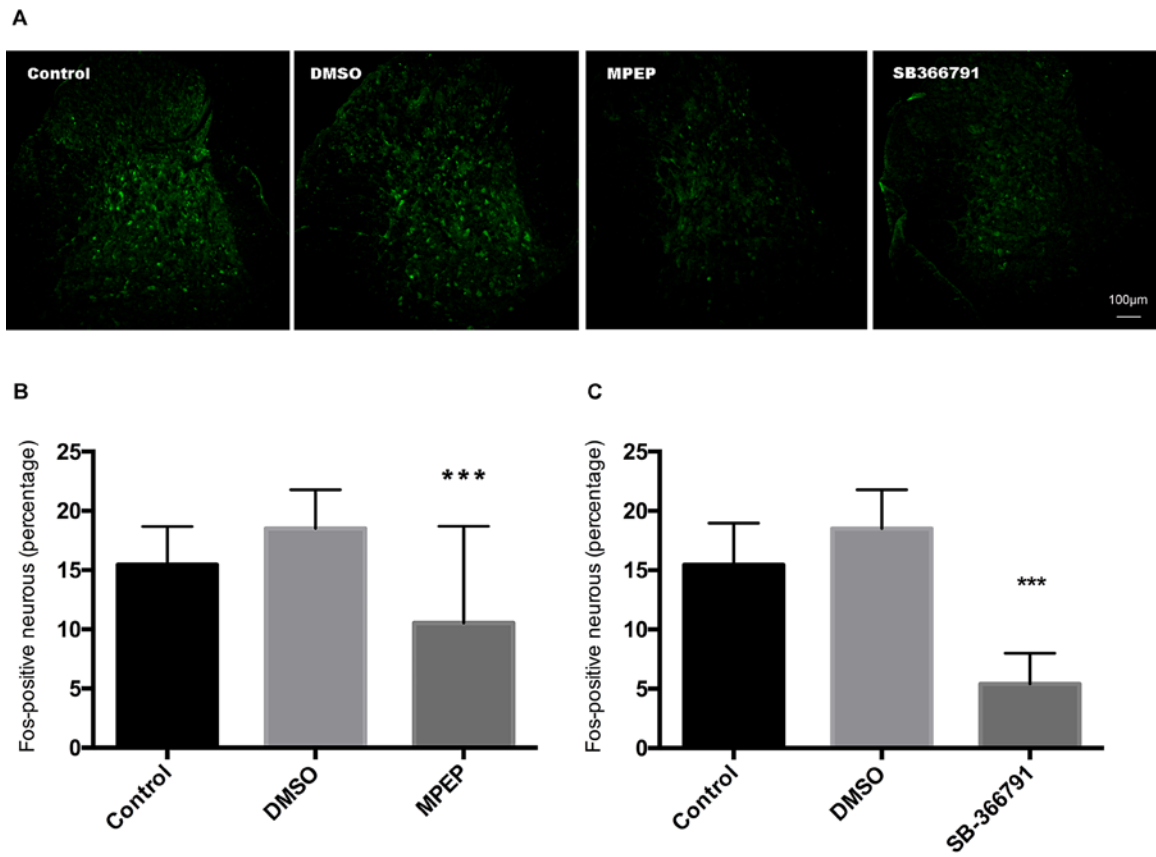


Figure 7

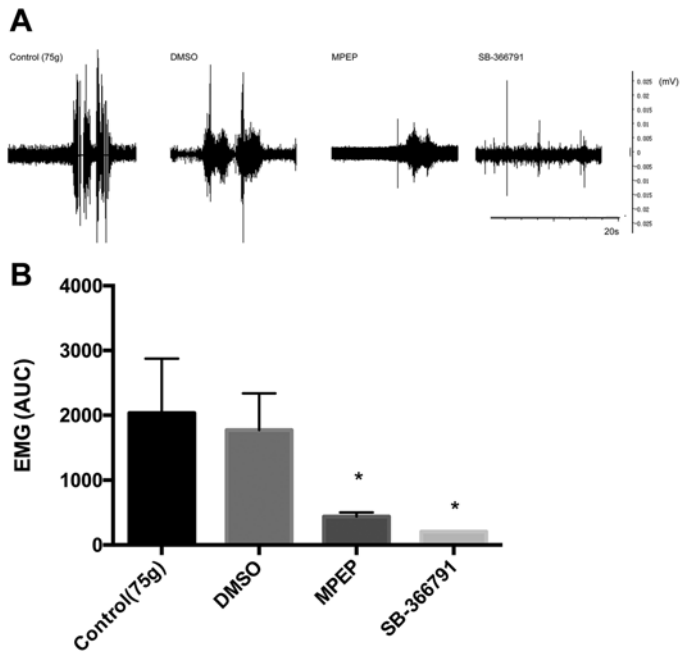


Figure 8

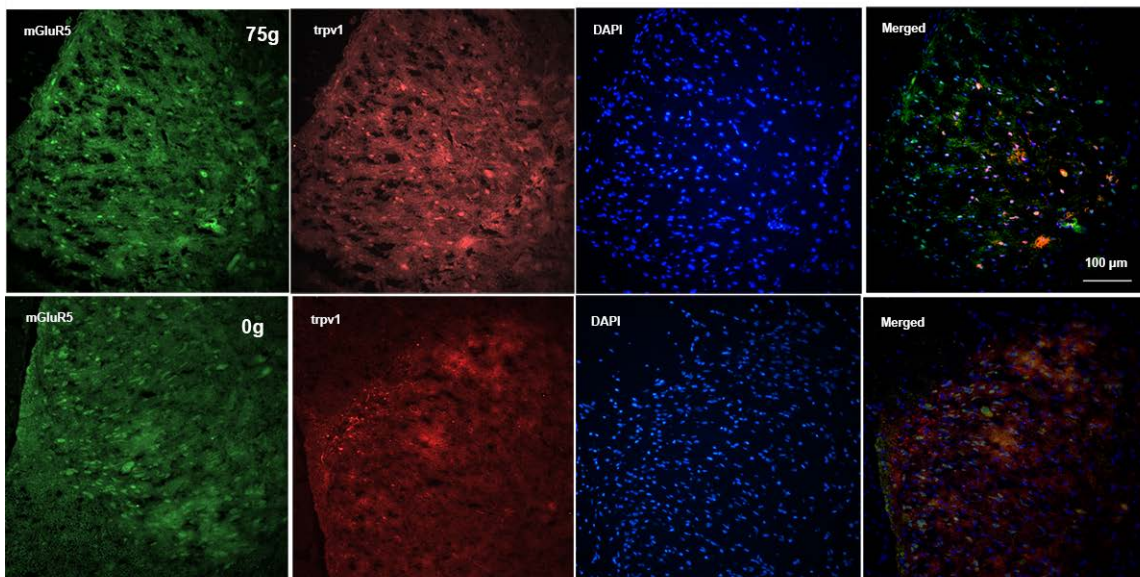


Figure 9

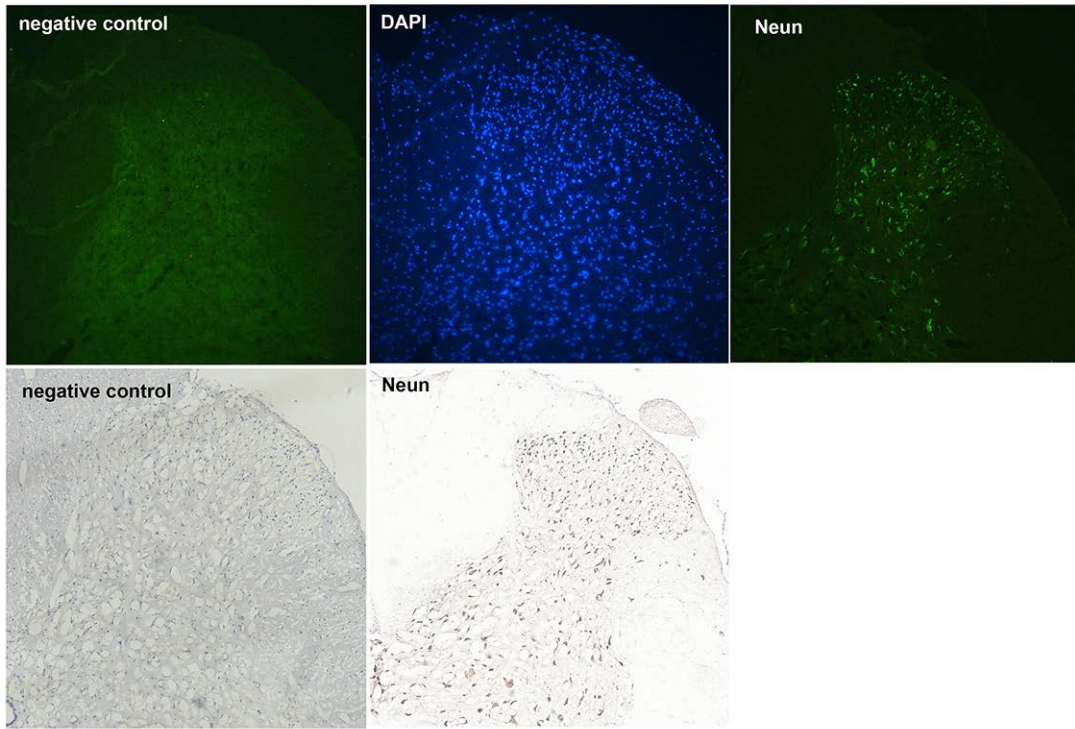


Figure 10

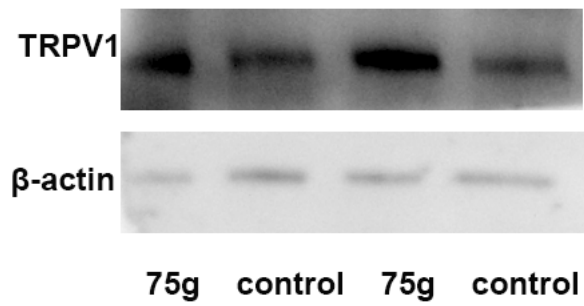


Figure 11

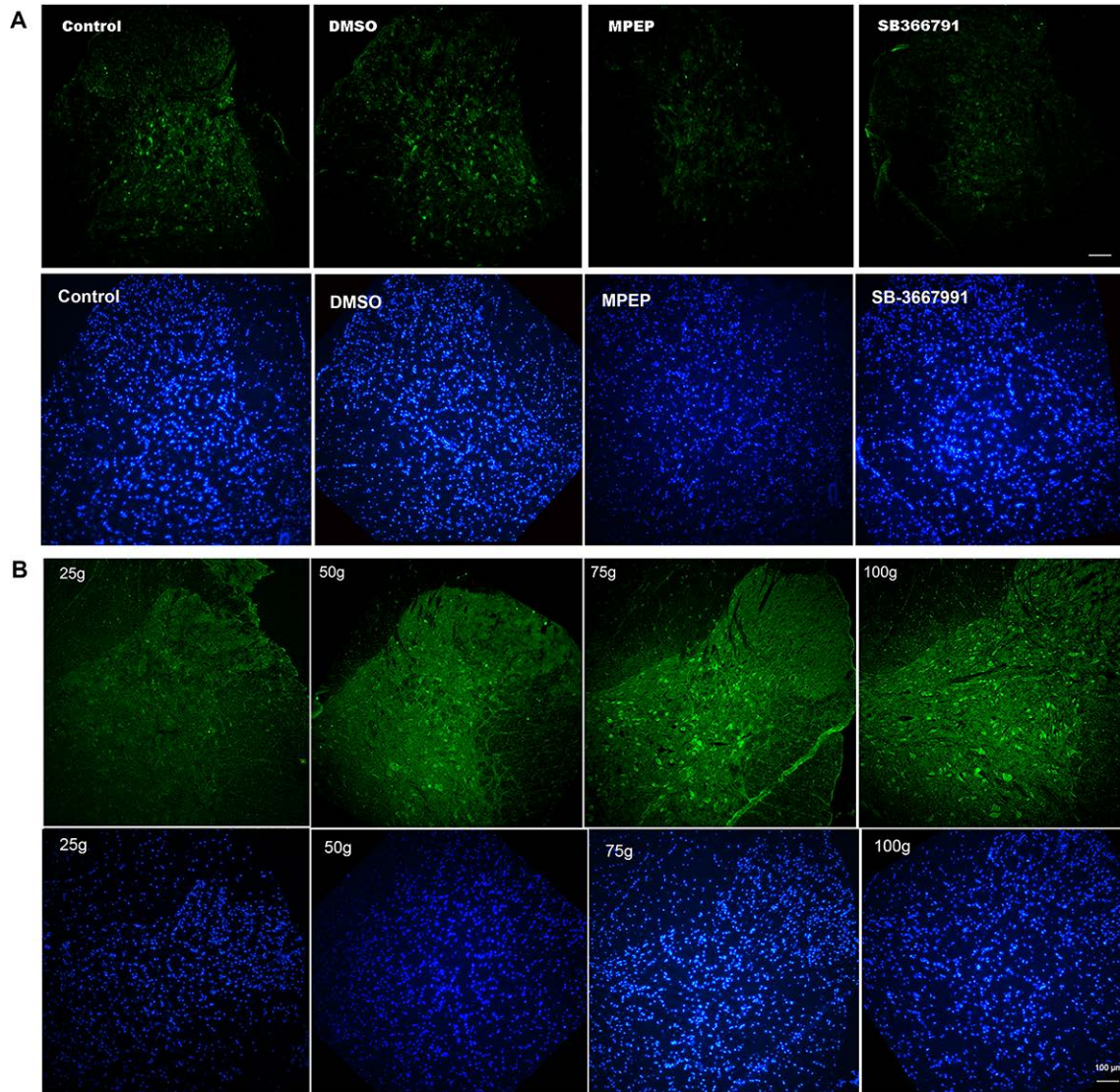


Figure 12